



The Accuracy of the Numerical Solution in Predicting Ahmed Body Components Drag Coefficients

Fatima-zahra Hachimy^{1,*}, Ashraf A. Omar¹, Omer Elsayed¹

¹ International University of Rabat, School of aerospace engineering, LERMA Lab, Campus UIR Parc Technopolis, Rocade, Rabat-Sale, 11100 - Sala Al Jadida, Maroc, Morocco

ARTICLE INFO

Article history:

Received 27 March 2022

Received in revised form 25 April 2022

Accepted 14 May 2022

Available online 31 May 2022

Keywords:

K-epsilon; K-omega SST; SST; ANSYS Fluent; AHMED BODY

ABSTRACT

In recent years, the aerodynamic drag became a major interest of automotive industry as it is one of the main components affecting the fuel consumption. To reduce aerodynamic drag force and improve the energetic efficiency, a complete understanding of the flow around ground vehicles is highly required. This study focused on the accuracy of a three different turbulence models in predicting Ahmed body components drag coefficients. Ahmed Body is a simplified model which mimics the bluff bodies in automotive aerodynamics. This study uses ANSYS Fluent to simulate the flow around Ahmed Body. Three different turbulence models (K-epsilon, K-omega SST and SST) were used in the study. The drag coefficient components for the different sections of the model were validated with the experimental published data. The results have shown that the SST model predicted accurately the total drag coefficient but failed to provide good agreement for the components drag coefficients.

1. Introduction

High fuel prices, growing concerns for the environmental effect of exhaust emissions, the depletion of fossil fuels greenhouse gas emissions, coupled with the need for continuous performance improvement for road cars and commercial vehicles, fueled an interest in optimizing fuel consumption. Aerodynamic drag and vehicle weight are recognized as the main sources of fuel consumption [1]. According to conducted research by Sudin *et al.*, [2], the aerodynamic drag of road vehicles by itself contributes up to 50 percent of the fuel consumed in highway speeds. More specifically, aerodynamic drag increases with the square of the vehicle velocity [3]. The aerodynamic drag for road vehicle is mainly pressure drag, which is caused by the vortex generation at the rear part.

To achieve a reduction in the aerodynamic drag or more specifically the pressure drags, it is necessary to use flow control mechanisms that can either prevent or delay separation at the rear part of road vehicles. The flow control techniques are classified as passive or active flow control. The active flow control systems require energy expenditures and usually involve automated control

* Corresponding author.

E-mail address: fatima-zahra.hachimy@uir.ac.ma (Fatima-zahra Hachimy)

process when the passive flow control techniques require no energy expenditure and usually are easy to implement to already existing designs.

Shankar and Devaradjane [4] have experimentally and numerically investigated the case of using 3 delta type of vortex generators for a sedan car at several yaw angles. The side VGs were moveable when the one in the middle were kept stationary. A maximum drag reduction of about 4.53% was achieved. Zakher *et al.*, [5] studied vortex generators added to a sedan car model and achieved a drag reduction of about 10% for Reynolds number larger than 96×10^5 . Kim *et al.*, [6] have experimentally tested the use of a bio-inspired flap on an Ahmed body model and the drag was reduced by 19%. Tian *et al.*, [7] have studied a configuration of flaps implemented to two Ahmed body models with different slant angles (25° and 35°). The maximum drag reduction achieved was 21%. Unni [8] have studied numerically the implementation of an underbody diffuser with flaps to a formula SAE car. An increase up to 25% in the down force have been achieved. Cho *et al.*, [9] have achieved a drag reduction of about 8.4% using three different devices, under-cover, under-fin and side air dam. Wahba *et al.*, [10] have used numerical simulation to investigate the use of guide vanes for two different ground vehicle models. The first model was a simple bus and the second one was a sport utility vehicle. They achieved a drag reduction of about 18 %.

To achieve pressure drag reduction, it is necessary to understand the flow behavior around ground vehicles and the vortex distribution. Ahmed body is a simplified car model with a moveable slant placed at the rear of the body and it was first introduced by Ahmed in the early 1980s [11]. The different angles of the slant plane serve to mimic the different vehicle types available on ground. The Ahmed body model becomes an important step in the automotive industry as a calibration for wind tunnels and validation for the numerical solution and turbulence models [12].

Many studies have been focusing on comparing the total drag coefficient with the experimental data without checking the component drag coefficients investigated in the benchmark case of Ahmed Body [11]. This study focuses on validating the results of the component drag coefficients from the numerical simulation with the experimental data.

This paper covers an investigation of the drag coefficient for the different parts of the Ahmed body model and the accuracy of three different turbulence models; K-epsilon, K-omega SST and SST in predicting components drag coefficient. Previously, Korkischko and Meneghini [12] have tested three different turbulence models: K-omega standard, K-omega SST and Spalart-Allmaras. They concluded that the K-omega SST had the best results for both steady and unsteady flow simulations.

2. CFD Method and Numerical Simulation

Like other industries, numerical simulation is a highly efficient method adopted in automotive industry to predict the aerodynamic behavior of the flow over the vehicles. Its effective analysis for the new designs and aerodynamic shapes provides a base for the designers before manufacturing. The analysis includes determining the forces applied on the body and the effect of flow separation and the wake region on the vehicle.

The CFD simulation is mainly composed of three parts: Pre-Processing, Solver and Post-Processing. The Solver is the core of the method as it is charged of solving the governing equations for each discrete volume using a turbulence model.

2.1 Governing Equations

Navier-Stokes equations are the fundamental equations governing the airflow over bodies for Computational Fluid Dynamics (CFD). The turbulent flow is characterized by a wide spectrum of vortex scales.

The Direct Numerical Simulation DNS is the ideal solution and can be accomplished by resolving all the vortex scales. However, Reynolds Averaged Navier Stokes RANS approach is more practical for engineering problems such as the flow over ground vehicles. The RANS approach is considered very promising as it resolves the large scales, while the small ones with less energy are modeled by specific sub-scale models.

$$\frac{\partial \rho U_i}{\partial x_i} = 0 \quad (1)$$

$$\frac{DU_i}{Dt} = g_i - \frac{1}{\rho} \frac{\partial P}{\partial x_i} + \frac{\partial}{\partial x_i} \left[\nu \left(\frac{\partial U_i}{\partial x_j} + \frac{\partial U_j}{\partial x_i} \right) - \overline{u_i u_j} \right] \quad (2)$$

$$\overline{u_i u_j} = \frac{2}{3} k \delta_{ij} - \nu_t \left(\frac{\partial U_i}{\partial x_j} + \frac{\partial U_j}{\partial x_i} \right) \quad (3)$$

3. Model Setup

The model used for the numerical simulation is Ahmed Body model (Figure 1) introduced by Ahmed *et al.*, [11] with a 25° rear slant angle. The model presents the essential aerodynamic features of the flow around road vehicles, and it is considered as an important step to select the suitable turbulence model in the numerical simulation for further studies.

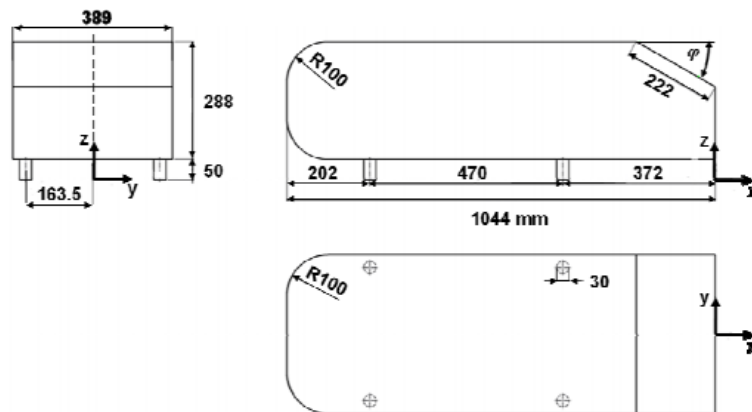


Fig. 1. Geometric model of Ahmed *et al.*, [13]

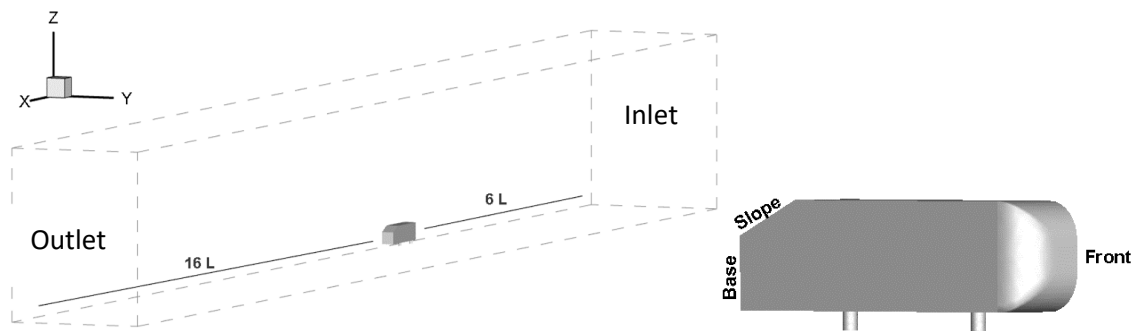


Fig. 2. Ahmed Body Design and Computational domain

The figures show the Ahmed Body designed with a slant angle of 25° and it was set in a domain with the following dimensions: $23L * 6W * 6W$ (Length*Width*Height; L length of the body and W the width) (see Figure 2).

The mesh is generated using the Mesh tool in ANSYS software, the grids were chosen coarse enough to reduce the computational effort and fine enough to resolve the flow. The distance of the first cell from the body surface is calculated by setting y^+ equal 50. Table 1 reports the parameters used during the mesh generation and Table 2 represents the results obtained from the grid independence test to ensure that the grid have no influence on the drag coefficient results.

Table 1
 Mesh parameters

Property	Parameter
Max. number of inflation layers	10
First layer thickness	4.63 e-004
Minimum element size	0.02
Growth rate	1.2
Total no. of elements	1,186,788

Table 2
 Grid independence results

Mesh	No. of cells	$C_{D_{total}}$
Course	379,997	0.295
Medium	571,247	0.289
Fine	1,186,788	0.282

To refine the mesh, a body of influence was used as a grid clustering at both sides of the Ahmed body. Inflation is also used next the body surface. The Figure 3 shows the mesh of the body as well as the domain.

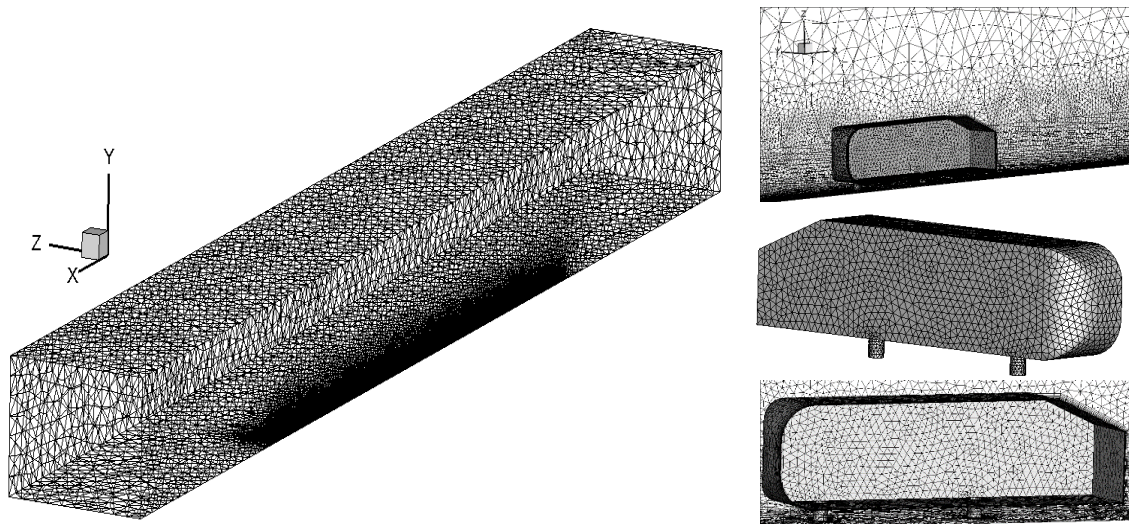


Fig. 3. Mesh Generation

The experimental drag coefficient data for a rear slant angle $\phi=25^\circ$ are presented in Table 2 [11]. The drag coefficient for the different sections shown in Table 2 presents total drag coefficient ($C_{D_{total}}$), Pressure drag coefficient (C_{D_p}), Viscous drag coefficient (C_r), drag coefficient for the front part of the body (C_k), drag coefficient for the base section (C_b) and the drag coefficient for the slant (C_s).

4. Results and Discussion

The simulation of the Ahmed Body model was first carried out using the K-epsilon turbulence model, then K-omega SST and SST (Shear Stress Transfer). The domain is split to proceed with half of the model as it is symmetrical and to reduce required computer memory. The inlet velocity is set to 40m/s and PRESTO method was used for pressure gradient. The flow characteristics was assumed steady and incompressible. The simulation was run until converged.

Table 3 represents the drag coefficients obtained using the three turbulent models. The result of the total drag coefficient of the SST model agrees well with the experiment with a difference of +0.82%. Other turbulence models present small deviation in predicting the total drag. From the results detailed in the Table 3, it can be noticed that the agreement of the total drag coefficient with the experimental value does not directly imply an accord between the drag coefficient components and the corresponding experimental data. Nevertheless, The SST model have the lowest differences for the components drag coefficient except for the base pressure drag coefficient C_b . K-epsilon model is noticed to be more accurate in predicting the base pressure drag coefficient.

Table 3
 Numerical results of drag coefficients

	Drag coefficient					
	$C_{D_{total}}$	C_{D_p}	C_r	C_k	C_b	C_s
Experimental [4]	0.28	-	0.052	0.0222	0.0726	0.136
K-epsilon	0.297	0.257	0.04	0.0478	0.08	0.108
Differences	5.72%	-	-27.50%	53.56%	9.25%	-25.93%
K-omega SST	0.2839	0.245	0.038	0.0399	0.0806	0.101
Differences	1.39%	-	-25.49%	79.73%	11.02%	-25.74%
SST	0.282	0.244	0.0374	0.03	0.082	0.0984
Differences	0.82%	-	-26.67%	35.14%	12.95%	-27.65%

There are many researchers who validated their numerical results using Ahmed body total drag coefficient without considering the section drag coefficients [14-17]. The total drag coefficient obtained in their results agrees well with the experimental data. However, the components drag coefficients were not investigated. Examining the total drag coefficient only is not sufficient to evaluate the accuracy of the turbulence models. As we have observed from Table 2, even if the total drag coefficient agrees with the experimental data, the components drag coefficients have large disagreement.

Figure 4 represents the pressure contour over the Ahmed Body model from different planes. It is shown that the pressure at the rear part of the body is low, and the large low-pressure zone distributed behind the body is the wake region. The difference of pressure between the front and the rear parts of the body is the main cause of the drag force for the road vehicle which is the pressured drag.

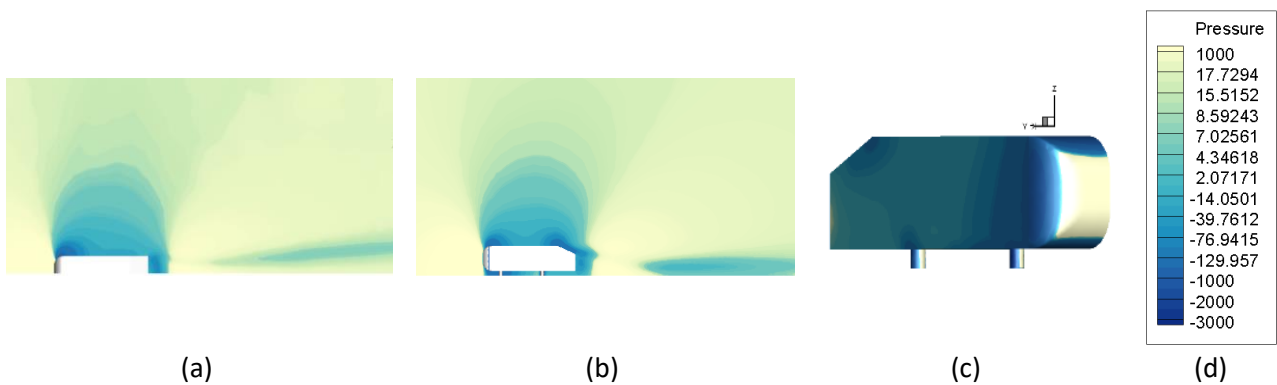


Fig. 4. Pressure contour (a) Top view (b) Around the body (c) Body surface

The wake region is also illustrated in Figure 5, the blue color represents low velocity magnitude in the x-direction as it is a recirculation area. The large distance of low velocity behind the Ahmed body model represents also the large low pressure area behind the body and emphasizes the difference of pressure behind the front and the back of the body causing high pressure drag.

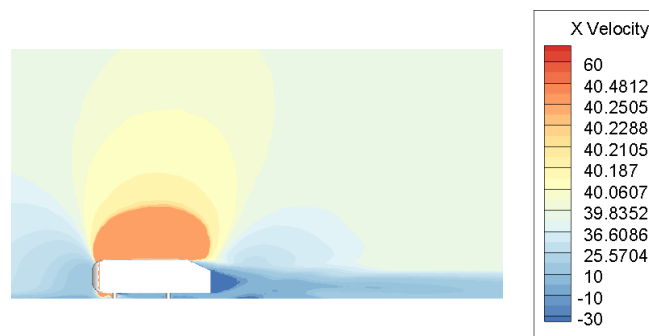


Fig. 5. x-direction Velocity magnitude contour

Figure 6 represents the tangent velocity vectors in different planes behind the studied body and illustrates the developing levels of the vortices after the flow separation on a 3m distance. As shown, the wake region is mainly composed of two vortices. The wake strength continues until attenuated after a large distance more than 3m. These vortices are the cause of the abrupt loss of pressure behind the Ahmed Body, and generally road vehicles.

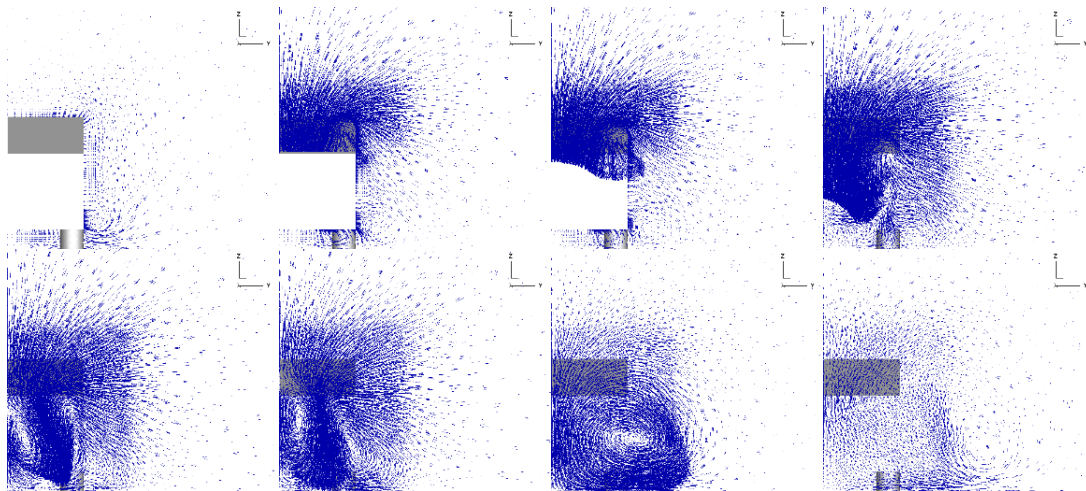


Fig. 6. The vortex development behind the Ahmed Body

Figure 7 and Figure 8 both shows the evaluation of the vortices behind the body on a large distance. They illustrate velocity contour (Figure 7) and Pressure contour (Figure 8) in different sections behind the studied body, which explains the importance of the resistance force due to difference of pressure.

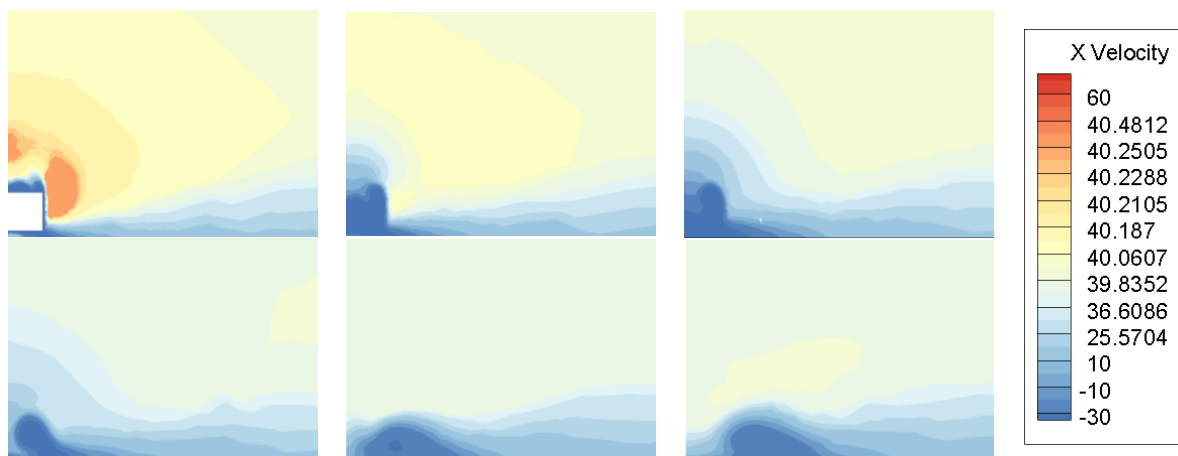


Fig. 7. Velocity magnitude contour for different zy-planes behind Ahmed Body ($x=-0,1; 5m$)

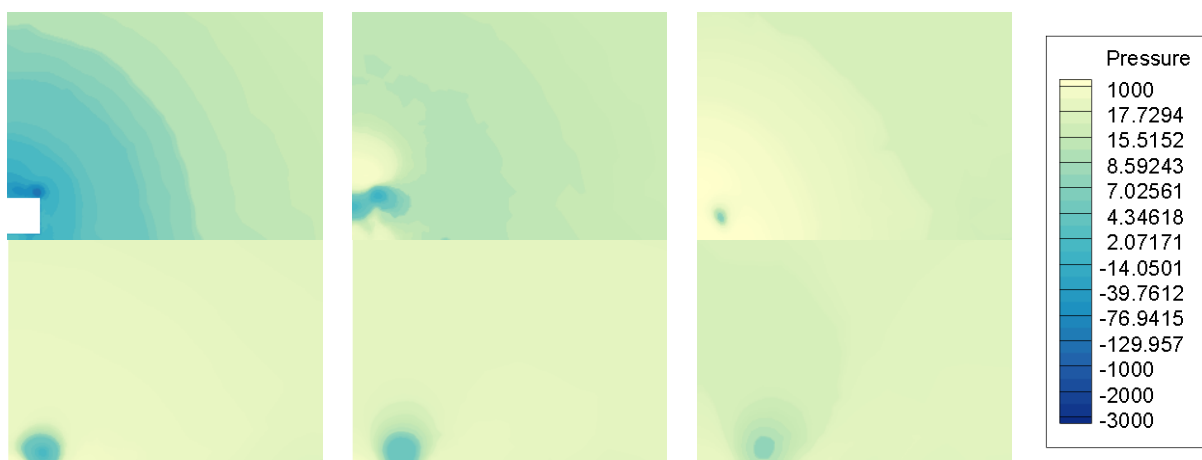


Fig. 8. Pressure contour for different zy-planes behind Ahmed Body ($x=-0,1; 5m$)

5. Conclusions

This paper discusses the accuracy of the three turbulent models (K-epsilon, K-omega SST and SST) in predicting and validating the components' drag coefficient with the experimental data presented by Ahmed *et al.*, [11]. From this work, the conclusion deduced can be as follows: The low pressure covering a large distance behind the vehicles is the major cause of the aerodynamic pressure drag. The agreement of the total drag coefficient with the experimental value does not imply the agreement of the components' drag coefficient with the experiment. The SST Model total drag coefficient have a good agreement with the experimental data. However, the base and slant drag coefficients are slightly higher than other used turbulence models.

Acknowledgement

This work is supported by the International University of Rabat (UIR). Many thanks to the LERMA laboratory for providing the In-house computing resources.

References

- [1] Mukut, A. N. M. Mominul Islam, and Mohammad Zoynal Abedin. "Review on aerodynamic drag reduction of vehicles." *International Journal of Engineering Materials and Manufacture* 4, no. 1 (2019): 1-14. <https://doi.org/10.26776/ijemm.04.01.2019.01>
- [2] Sudin, Mohd Nizam, Mohd Azman Abdullah, Shamsul Anuar Shamsuddin, Faiz Redza Ramli, and Musthafah Mohd Tahir. "Review of research on vehicles aerodynamic drag reduction methods." *International Journal of Mechanical and Mechatronics Engineering* 14, no. 02 (2014): 37-47.
- [3] Lee, Sang Wook. "Computational analysis of air jet wheel deflector for aerodynamic drag reduction of road vehicle." *Microsystem Technologies* 24, no. 11 (2018): 4453-4463. <https://doi.org/10.1007/s00542-018-3992-1>
- [4] Shankar, G., and G. Devaradjane. "Experimental and computational analysis on aerodynamic behavior of a car model with vortex generators at different yaw angles." *Journal of Applied Fluid Mechanics* 11, no. 1 (2018): 285-295. <https://doi.org/10.29252/jafm.11.01.28357>
- [5] Zakher, Bassem Nashaat, Mostafa El-Hadary, and Andrew Nabil Aziz. "The Effect of Vortex Generators on Aerodynamics for Sedan Cars." *CFD Letters* 11, no. 6 (2019): 1-17.
- [6] Kim, Dongri, Hoon Lee, Wook Yi, and Haecheon Choi. "A bio-inspired device for drag reduction on a three-dimensional model vehicle." *Bioinspiration & Biomimetics* 11, no. 2 (2016): 026004. <https://doi.org/10.1088/1748-3190/11/2/026004>
- [7] Tian, Jie, Yingchao Zhang, Hui Zhu, and Hongwei Xiao. "Aerodynamic drag reduction and flow control of Ahmed body with flaps." *Advances in Mechanical Engineering* 9, no. 7 (2017): 1687814017711390. <https://doi.org/10.1177/1687814017711390>
- [8] Unni, T. P. Aniruddhan. *Numerical Investigation on Aerodynamic Effects of Vanes and Flaps on Automotive Underbody Diffusers*. No. 2017-01-2163. SAE Technical Paper, 2017. <https://doi.org/10.4271/2017-01-2163>
- [9] Cho, Junho, Tae-Kyung Kim, Kyu-Hong Kim, and Kwanjung Yee. "Comparative investigation on the aerodynamic effects of combined use of underbody drag reduction devices applied to real sedan." *International Journal of Automotive Technology* 18, no. 6 (2017): 959-971. <https://doi.org/10.1007/s12239-017-0094-5>
- [10] Wahba, E. M., Humaid Al-Marzooqi, Majd Shaath, Mohamed Shahin, and Tarek El-Dhmashawy. "Aerodynamic drag reduction for ground vehicles using lateral guide vanes." *CFD Letters* 4, no. 2 (2012): 68-79.
- [11] Ahmed, Syed R., G. Ramm, and Gunter Faltin. "Some salient features of the time-averaged ground vehicle wake." *SAE Transactions* (1984): 473-503. <https://doi.org/10.4271/840300>
- [12] Korkischko, Ivan, and Julio Romano Meneghini. "Experimental investigation and numerical simulation of the flow around an automotive model: Ahmed body." In *Proceedings of COBEM*. ABCM, Brasília, 2007.
- [13] Hinterberger, Christof, M. Garcia-Villalba, and W. Rodi. "Large eddy simulation of flow around the Ahmed body." In *The Aerodynamics of Heavy Vehicles: Trucks, Buses, and Trains*, pp. 77-87. Springer, Berlin, Heidelberg, 2004. https://doi.org/10.1007/978-3-540-44419-0_7
- [14] Igali, Dastan, Olzhas Mukhmetov, Yong Zhao, Sai Cheong Fok, and Soo Lee Teh. "Comparative analysis of turbulence models for automotive aerodynamic simulation and design." *International Journal of Automotive Technology* 20, no. 6 (2019): 1145-1152. <https://doi.org/10.1007/s12239-019-0107-7>
- [15] Altaf, Alaman, Ashraf A. Omar, and Waqar Asrar. "Review of passive drag reduction techniques for bluff road

- vehicles." *IJUM Engineering Journal* 15, no. 1 (2014): 61-69. <https://doi.org/10.31436/iiumej.v15i1.477>
- [16] Mosiężny, Jędrzej, Bartosz Ziegler, Przemysław Grzymisławski, and Rafał Ślefarski. "Base drag reduction concept for commercial road vehicles." *Energy* 205 (2020): 118075. <https://doi.org/10.1016/j.energy.2020.118075>
- [17] Mohammadikalakoo, Babak, Paolo Schito, and Mahmoud Mani. "Passive flow control on Ahmed body by rear linking tunnels." *Journal of Wind Engineering and Industrial Aerodynamics* 205 (2020): 104330. <https://doi.org/10.1016/j.jweia.2020.104330>